# A dual formulation for time-domain wavefield reconstruction inversion

**Gabrio Rizzuti**[*,1], Mathias Louboutin[1], Rongrong Wang[2], Emmanouil Daskalakis[3], and Felix J. Herrmann[1]

[1] Georgia Institute of Technology
[2] Michigan State University
[3] Vancouver Community College

SLIM

SEG
San Antonio
09/18/2019

# PDE-constrained optimization

$$\min_{\mathbf{m},\mathbf{u}} \frac{1}{2}||\mathbf{d} - R\,\mathbf{u}||^2 \quad \text{subject to} \quad A(\mathbf{m})\,\mathbf{u} = \mathbf{q}$$

Vectors:

| | |
|---|---|
| $\mathbf{d}$ | data |
| $\mathbf{q}$ | source |
| $\mathbf{m}$ | model |
| $\mathbf{u}$ | wavefield |

Operators:

| | |
|---|---|
| $A(\mathbf{m})$ | wave equation |
| $R$ | receiver restriction |

# PDE-constrained optimization (all-at-once full-space)

$$\max_{\mathbf{v}} \min_{\mathbf{m},\mathbf{u}} \mathcal{L}(\mathbf{m},\mathbf{u},\mathbf{v}), \quad \mathcal{L}(\mathbf{m},\mathbf{u},\mathbf{v}) = \frac{1}{2}||\mathbf{d} - R\,\mathbf{u}||^2 + \langle \mathbf{v}, \mathbf{q} - A(\mathbf{m})\,\mathbf{u} \rangle$$

[Haber, E., and Ascher, U. M., 2001; Biros, G., and Ghattas, O., 2005; Grote et al, 2011]

Pros:

✓ **cheap** evaluation and gradient computation (no need for PDE solution)

Cons:

✘ **need simultaneous storage of wavefields and multipliers**
(for each source and time/frequency sample)

# PDE-constrained optimization (reduced space)

$$\min_{\mathbf{m}} J(\mathbf{m}), \quad J(\mathbf{m}) = \frac{1}{2}||\mathbf{d} - F(\mathbf{m})\,\mathbf{q}||^2, \quad F(\mathbf{m}) = R\,A(\mathbf{m})^{-1}$$

[Tarantola, A., ‘84; Haber, E., et al, 2000; Epanomeritakis, I., et al, 2008]

Pros:

✓ no simultaneous **wavefield storage** for all sources and frequencies (compute and discard)

Cons:

✘ highly **non-convex** (needs good starting model)

✘ requires exact **PDE solutions** (prohibitive in 3D for frequency domain)

# PDE-constrained optimization (penalty method)

$$J_\lambda(\mathbf{m}, \mathbf{u}) = \frac{1}{2}||\mathbf{d} - R\,\mathbf{u}||^2 + \frac{\lambda^2}{2}\underbrace{||\mathbf{q} - A(\mathbf{m})\,\mathbf{u}||^2}_{\text{PDE penalty}}$$

[van den Berg, P. M., and Kleinman, R. E., 1997; van Leeuwen, T. and Herrmann, F. J., 2013]

# PDE-constrained optimization (WRI)

$$J_{\lambda}(\mathbf{m}) = \frac{1}{2}||\mathbf{d} - R\,\bar{\mathbf{u}}||^2 + \frac{\lambda^2}{2}||\mathbf{f} - A(\mathbf{m})\,\bar{\mathbf{u}}||^2$$

[van Leeuwen, T. and Herrmann, F. J., 2013]

$$\begin{bmatrix} R \\ \lambda A(\mathbf{m}) \end{bmatrix} \bar{\mathbf{u}} = \begin{bmatrix} \mathbf{d} \\ \lambda \mathbf{q} \end{bmatrix}$$

augmented wave equation

Pros:

✓ no simultaneous **wavefield storage** for all sources and frequencies (compute and discard)

Cons:

✘ needs **augmented PDE solution**

**frequency** domain: does not effectively scale to 3D

**time** domain: no explicit time-marching scheme

# Early attempt to circumvent WRI shortcomings

$$J_\lambda(\mathbf{m}) = \frac{1}{2}||\mathbf{d} - F(\mathbf{m})\,\bar{\mathbf{q}}||^2 + \frac{\lambda^2}{2}||\mathbf{q} - \bar{\mathbf{q}}||^2$$

[Wang et al, 2016, Huang et al, 2018]:

$$\begin{bmatrix} F(\mathbf{m}) \\ \lambda I \end{bmatrix} \bar{\mathbf{q}} = \begin{bmatrix} \mathbf{d} \\ \lambda \mathbf{q} \end{bmatrix}$$

augmented wave equation

Variable projection **approximation**:

$$\bar{\mathbf{q}} \approx \mathbf{q} + \frac{1}{\lambda^2} F(\mathbf{m})^* (\mathbf{d} - F(\mathbf{m})\,\mathbf{q}), \quad \lambda \to \infty$$

# Denoising reformulation of WRI

$$\min_{\mathbf{m},\mathbf{u}} \frac{1}{2}\underbrace{||\mathbf{q} - A(\mathbf{m})\,\mathbf{u}||^2}_{\text{PDE misfit}} \quad \text{s.t.} \quad \underbrace{||\mathbf{d} - R\,\mathbf{u}|| \leq \varepsilon}_{\text{data constraint}}$$

[Wang, R., and Herrmann, F. J., 2017]

# Dual formulation of WRI - Lagrangian

$$\min_{\mathbf{m},\mathbf{u}} \underbrace{\frac{1}{2}||\mathbf{q} - A(\mathbf{m})\,\mathbf{u}||^2}_{\text{PDE misfit}} \quad \text{s.t.} \quad \underbrace{||\mathbf{d} - R\,\mathbf{u}|| \leq \varepsilon}_{\text{data constraint}}$$

Saddle-point problem:

$$\max_{\mathbf{y}} \min_{\mathbf{m},\mathbf{u}} \mathcal{L}(\mathbf{m}, \mathbf{u}, \mathbf{y})$$

$$\mathcal{L}(\mathbf{m}, \mathbf{u}, \mathbf{y}) = \frac{1}{2}||\mathbf{q} - A(\mathbf{m})\,\mathbf{u}||^2 + \langle \mathbf{y}, \mathbf{d} - R\,\mathbf{u} \rangle - \varepsilon||\mathbf{y}||$$

# Dual formulation of WRI – Augmented wave equation

Solving for **u** ...

$$A(\mathbf{m})\,\bar{\mathbf{u}} = \mathbf{q} + F(\mathbf{m})^*\,\mathbf{y}$$

augmented wave equation

Saddle-point problem:

$$\max_{\mathbf{y}} \min_{\mathbf{m},\mathbf{u}} \mathcal{L}(\mathbf{m},\mathbf{u},\mathbf{y}) = \max_{\mathbf{y}} \min_{\mathbf{m}} \mathcal{L}(\mathbf{m},\bar{\mathbf{u}},\mathbf{y})$$

$$\mathcal{L}(\mathbf{m},\mathbf{u},\mathbf{y}) = \frac{1}{2}||\mathbf{q} - A(\mathbf{m})\,\mathbf{u}||^2 + \langle \mathbf{y}, \mathbf{d} - R\,\mathbf{u} \rangle - \varepsilon||\mathbf{y}||$$

# Dual formulation of WRI – Objective and gradients

Dual saddle-point formulation (= after **u** substitution):

$$\max_{\mathbf{y}} \min_{\mathbf{m}} \bar{\mathcal{L}}(\mathbf{m}, \mathbf{y})$$

$$\bar{\mathcal{L}}(\mathbf{m}, \mathbf{y}) = -\frac{1}{2}||F(\mathbf{m})^* \, \mathbf{y}||^2 + \langle \mathbf{y}, \mathbf{d} - F(\mathbf{m}) \, \mathbf{q} \rangle - \varepsilon ||\mathbf{y}||$$

Gradients:

$$\nabla_{\mathbf{m}} \bar{\mathcal{L}} = -\mathrm{D} \, F(\mathbf{m}, \mathbf{q} + F(\mathbf{m})^* \, \mathbf{y})^* \, \mathbf{y}$$

similar to conventional FWI gradient

$$\nabla_{\mathbf{y}} \bar{\mathcal{L}} = \mathbf{d} - F(\mathbf{m}) \, (\mathbf{q} + F(\mathbf{m})^* \, \mathbf{y}) - \varepsilon \mathbf{y} / ||\mathbf{y}||$$

generalized-source data residual
+ relaxation term

# Dual formulation of WRI (recap)

Dual saddle-point formulation:

$$\max_{\mathbf{y}} \min_{\mathbf{m}} \bar{\mathcal{L}}(\mathbf{m}, \mathbf{y})$$

$$\bar{\mathcal{L}}(\mathbf{m}, \mathbf{y}) = -\frac{1}{2}||F(\mathbf{m})^* \, \mathbf{y}||^2 + \langle \mathbf{y}, \mathbf{d} - F(\mathbf{m})\, \mathbf{q} \rangle - \varepsilon ||\mathbf{y}||$$

Obtained **model extension** along **data space**: $\bar{\mathcal{L}} : M \times D \to \mathbb{R}$

Pros:

✓ amenable to **time-domain** methods

✓ extra variable **storage is affordable**

Cons:

✘ extra **time complexity** (2x PDE solutions wrt FWI)

✘ non trivial **optimization strategy**

# Other issues (1): Dual variable scaling

Dual saddle-point formulation:

$$\max_{\mathbf{y}} \min_{\mathbf{m}} \bar{\mathcal{L}}(\mathbf{m}, \mathbf{y})$$

$$\bar{\mathcal{L}}(\mathbf{m}, \mathbf{y}) = -\frac{1}{2}||F(\mathbf{m})^* \, \mathbf{y}||^2 + \langle \mathbf{y}, \mathbf{d} - F(\mathbf{m}) \, \mathbf{q} \rangle - \varepsilon ||\mathbf{y}||$$

$$A(\mathbf{m}) \, \bar{\mathbf{u}} = \mathbf{q} + \alpha \, F(\mathbf{m})^* \, \mathbf{y}$$

**unbalanced contributions** of physical and augmented sources

# Other issues (1): Dual variable scaling

Dual saddle-point formulation:

$$\max_{\mathbf{y}} \min_{\mathbf{m}} \bar{\mathcal{L}}(\mathbf{m},\mathbf{y})$$

$$\bar{\mathcal{L}}(\mathbf{m},\mathbf{y}) = -\frac{1}{2}||F(\mathbf{m})^*\,\mathbf{y}||^2 + \langle \mathbf{y}, \underbrace{\mathbf{d} - F(\mathbf{m})\,\mathbf{q}}_{\mathbf{r}} \rangle - \varepsilon||\mathbf{y}||$$

**r**: data residual

Solving for the scaling parameter...

$$\bar{\bar{\mathcal{L}}}(\mathbf{m},\mathbf{y},\alpha) := \bar{\mathcal{L}}(\mathbf{m},\alpha\mathbf{y})$$

$$\bar{\bar{\mathcal{L}}}(\mathbf{m},\mathbf{y}) := \max_{\alpha} \bar{\bar{\mathcal{L}}}(\mathbf{m},\mathbf{y},\alpha) = \bar{\bar{\mathcal{L}}}(\mathbf{m},\mathbf{y},\bar{\alpha})$$ (variable projection!)

$$\bar{\alpha} = \begin{cases} \mathrm{sign}(\langle \mathbf{y},\mathbf{r}\rangle)\dfrac{|\langle \mathbf{y},\mathbf{r}\rangle| - \varepsilon||\mathbf{y}||}{||F(\mathbf{m})^*\,\mathbf{y}||^2}, & |\langle \mathbf{y},\mathbf{r}\rangle| \geq \varepsilon||\mathbf{y}|| \\ 0, & \text{otherwise} \end{cases}$$

# Other issues (1): Dual variable scaling

Dual saddle-point formulation (scaled):

$$\max_{\mathbf{y}} \min_{\mathbf{m}} \bar{\bar{\mathcal{L}}}(\mathbf{m}, \mathbf{y})$$

$$\bar{\bar{\mathcal{L}}}(\mathbf{m}, \mathbf{y}) = \begin{cases} \frac{1}{2}(|\langle \hat{\mathbf{y}}, \mathbf{r} \rangle| - \varepsilon ||\hat{\mathbf{y}}||)^2, & |\langle \hat{\mathbf{y}}, \mathbf{r} \rangle| \geq \varepsilon ||\hat{\mathbf{y}}|| \\ 0, & \text{otherwise} \end{cases} \quad \left( \hat{\mathbf{y}} = \frac{\mathbf{y}}{||F(\mathbf{m})^* \mathbf{y}||} \right)$$

Gradients:

$$\nabla_{\mathbf{m}} \bar{\bar{\mathcal{L}}} = \nabla_{\mathbf{m}} \bar{\mathcal{L}}(\mathbf{m}, \bar{\alpha}\mathbf{y})$$

$$\nabla_{\mathbf{y}} \bar{\bar{\mathcal{L}}} = \bar{\alpha} \nabla_{\mathbf{y}} \bar{\mathcal{L}}(\mathbf{m}, \bar{\alpha}\mathbf{y})$$

# Other issues (2): Optimization strategy

Theoretical/numerical studies evidence:

- ✘ **alternating update** approach: ineffective
- ✘ **variable projection for y** (fixed m) = WRI: expensive

$$F(\mathbf{m})\,F(\mathbf{m})^*\,\bar{\mathbf{y}} + \varepsilon\,\bar{\mathbf{y}}/||\bar{\mathbf{y}}|| = \mathbf{r}(\mathbf{m})$$

# Other issues (2): Optimization strategy

Theoretical/numerical studies evidence:

- ✘ **alternating update** approach: ineffective
- ✘ **variable projection for y** (fixed m) = WRI: expensive

$$F(\mathbf{m})\, F(\mathbf{m})^*\, \bar{\mathbf{y}} + \varepsilon\, \bar{\mathbf{y}}/||\bar{\mathbf{y}}|| = \mathbf{r}(\mathbf{m})$$

$$\bar{\mathcal{L}}_\varepsilon(\mathbf{m},\mathbf{y}) = -\frac{1}{2}||F(\mathbf{m})^*\,\mathbf{y}||^2 + \langle \mathbf{y}, \mathbf{r}(\mathbf{m})\rangle - \varepsilon||\mathbf{y}||$$

$$\bar{\mathcal{L}}_\lambda(\mathbf{m},\mathbf{y}) = -\frac{1}{2}||F(\mathbf{m})^*\,\mathbf{y}||^2 + \langle \mathbf{y}, \mathbf{r}(\mathbf{m})\rangle - \frac{\lambda^2}{2}||\mathbf{y}||^2$$

To avoid non-linear system in **y**

# Other issues (2): Optimization strategy

Theoretical/numerical studies evidence:

✓ **y** ≈ **r** data residual cheap approximation of the optimal y

Reduced formulation:

$$\min_{\mathbf{m}} \bar{\bar{\bar{\mathcal{L}}}}(\mathbf{m})$$

$$\bar{\bar{\bar{\mathcal{L}}}}(\mathbf{m}) = \bar{\bar{\mathcal{L}}}(\mathbf{m}, \mathbf{r}(\mathbf{m})) \quad \left[ = \frac{1}{2} \frac{||\mathbf{r}||^2}{||F(\mathbf{m})^* \, \mathbf{r}||^2} \left(||\mathbf{r}|| - \varepsilon\right)^2 \right]$$

See also [van Leeuwen, 2019]

Gradient:

$$\nabla_{\mathbf{m}} \bar{\bar{\bar{\mathcal{L}}}} = \nabla_{\mathbf{m}} \bar{\bar{\mathcal{L}}}(\mathbf{m}, \mathbf{r}) - \boxed{D\,F(\mathbf{m}, \mathbf{q})^* \nabla_{\mathbf{y}} \bar{\bar{\mathcal{L}}}(\mathbf{m}, \mathbf{r})}$$

# Other issues (2): Optimization strategy

Theoretical/numerical studies evidence:

✓ **y** ≈ **r** data residual cheap approximation of the optimal y

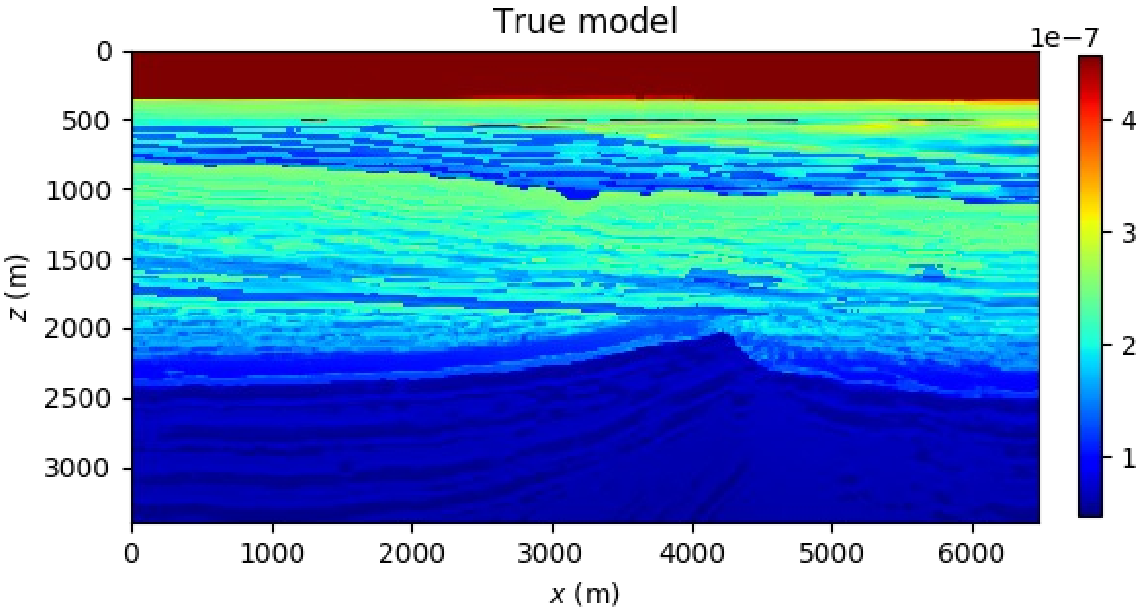

# Other issues (2): Optimization strategy

Theoretical/numerical studies evidence:

✓ **y** ≈ **r** data residual cheap approximation of the optimal y

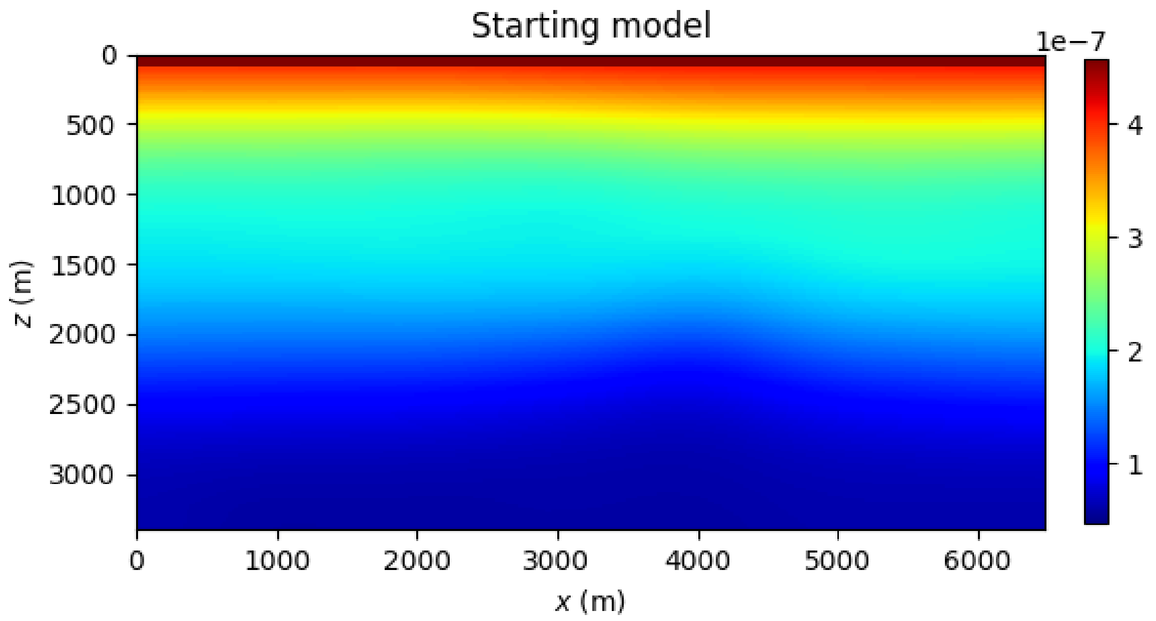

# Other issues (2): Optimization strategy

Theoretical/numerical studies evidence:

✓ **y** ≈ **r** data residual cheap approximation of the optimal y

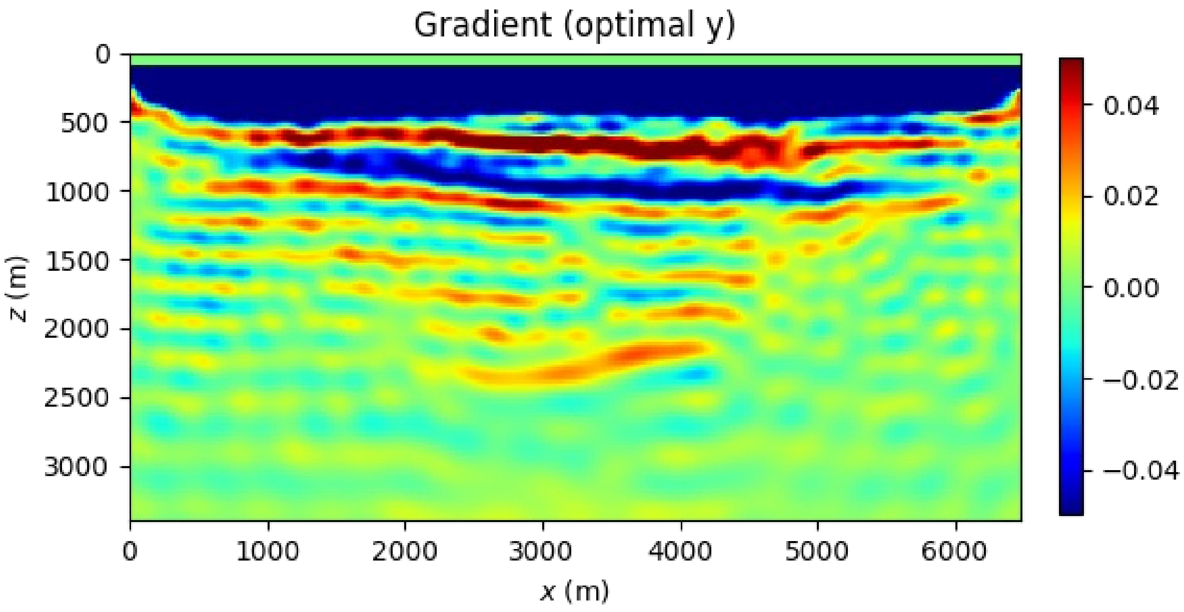

# Other issues (2): Optimization strategy

Theoretical/numerical studies evidence:

✓ **y** ≈ **r** data residual cheap approximation of the optimal y

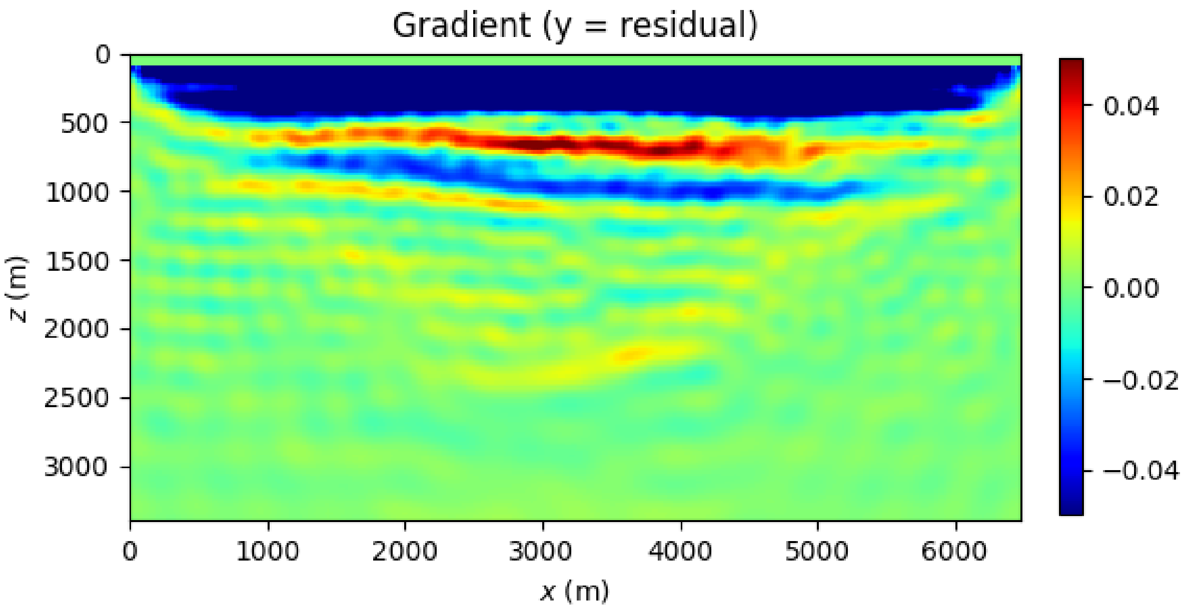

# Other issues (2): Optimization strategy

Theoretical/numerical studies evidence:

✓ **y** ≈ **r** data residual cheap approximation of the optimal y

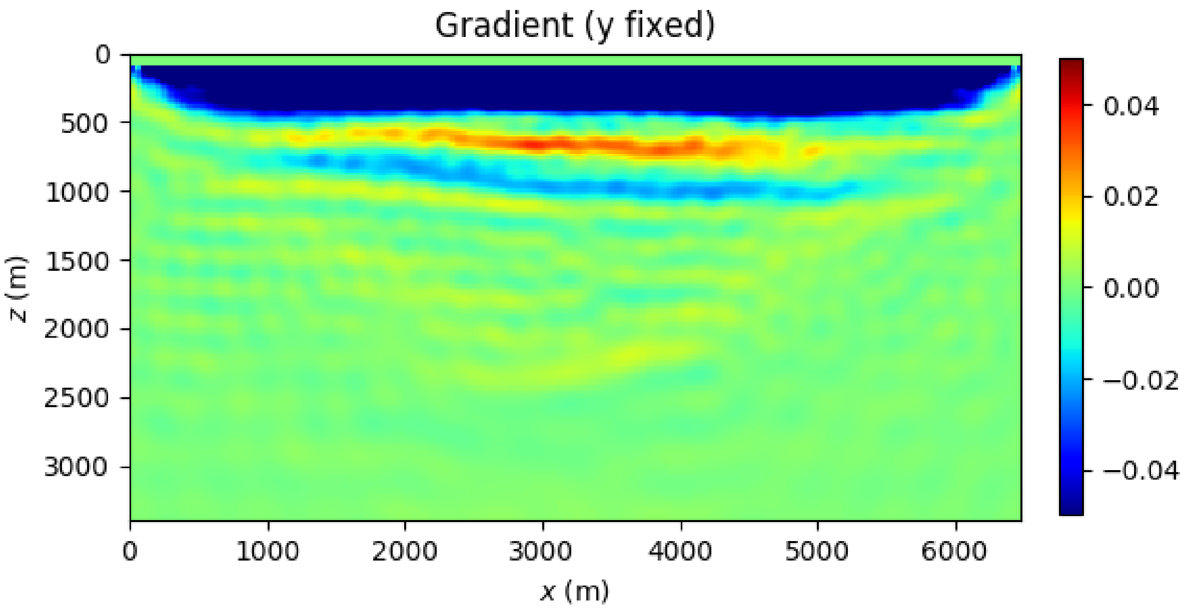

# Other issues (3): Weighted PDE misfit

Yet another important theme!

- prior information about source position: **weighted PDE misfit** ([Huang et al, 2018]):

$$\min_{\mathbf{m},\mathbf{u}} \frac{1}{2}||\mathbf{q} - A(\mathbf{m})\,\mathbf{u}||_W^2 \quad \text{s.t.} \quad ||\mathbf{d} - R\,\mathbf{u}|| \leq \varepsilon$$

$$||\mathbf{u}||_W^2 := \langle W^{-1}\mathbf{u}, \mathbf{u}\rangle, \qquad W^{-1} = \text{diag}(\mathbf{w}^{-1}),\ \mathbf{w}^{-1}(\mathbf{x};\mathbf{x}_s) = \frac{||\mathbf{x} - \mathbf{x}_s||^2 + \delta^2}{\delta^2}$$

# Other issues (3): Weighted PDE misfit

Yet another important theme!

- prior information about source position: **weighted PDE misfit** ([Huang et al, 2018]):

$$\bar{\mathcal{L}}_W(\mathbf{m},\mathbf{y}) = -\frac{1}{2}||\,F(\mathbf{m})^*\,\mathbf{y}||^2_{W^{-1}} + \langle \mathbf{y}, \mathbf{r}(\mathbf{m})\rangle - \varepsilon||\mathbf{y}||$$

$$||\mathbf{u}||^2_{W^{-1}} := \langle W\mathbf{u},\mathbf{u}\rangle, \qquad W = \mathrm{diag}(\mathbf{w}),\ \mathbf{w}(\mathbf{x};\mathbf{x}_s) = \frac{\delta^2}{||\mathbf{x}-\mathbf{x}_s||^2+\delta^2}$$

# Other issues (3): Weighted PDE misfit

Yet another important theme!

- prior information about source position: **weighted PDE misfit** ([Huang et al, 2018]):

$$\min_{\mathbf{m},\mathbf{u}} ||\mathbf{q} - A(\mathbf{m})\,\mathbf{u}||_{1,W} \quad \text{s.t.} \quad ||\mathbf{d} - R\,\mathbf{u}|| \leq \varepsilon$$ (alternatively)

$$||\mathbf{u}||_{1,W} := ||W^{-1/2}\mathbf{u}||_1$$

# Other issues (3): Weighted PDE misfit

Yet another important theme!

- prior information about source position: **weighted PDE misfit** ([Huang et al, 2018]):

$$\min_{\mathbf{m},\mathbf{u}} ||\mathbf{q} - A(\mathbf{m})\,\mathbf{u}||_{1,W} + \frac{1}{2\mu}||\mathbf{q} - A(\mathbf{m})\,\mathbf{u}||_{2,W}^2 \quad \text{s.t.} \quad ||\mathbf{d} - R\,\mathbf{u}|| \leq \varepsilon$$

$$||\mathbf{u}||_{1,W} := ||W^{-1/2}\mathbf{u}||_1$$

similarly to [Sharan et al, 2019]

# Numerical examples

**Caveat**:

inversion experiments carried out in the **frequency domain:**

- computational convenience
- fair comparison with conventional WRI (only feasible in frequency domain)

# Numerical examples – Gaussian lens [Huang et al, 2018]

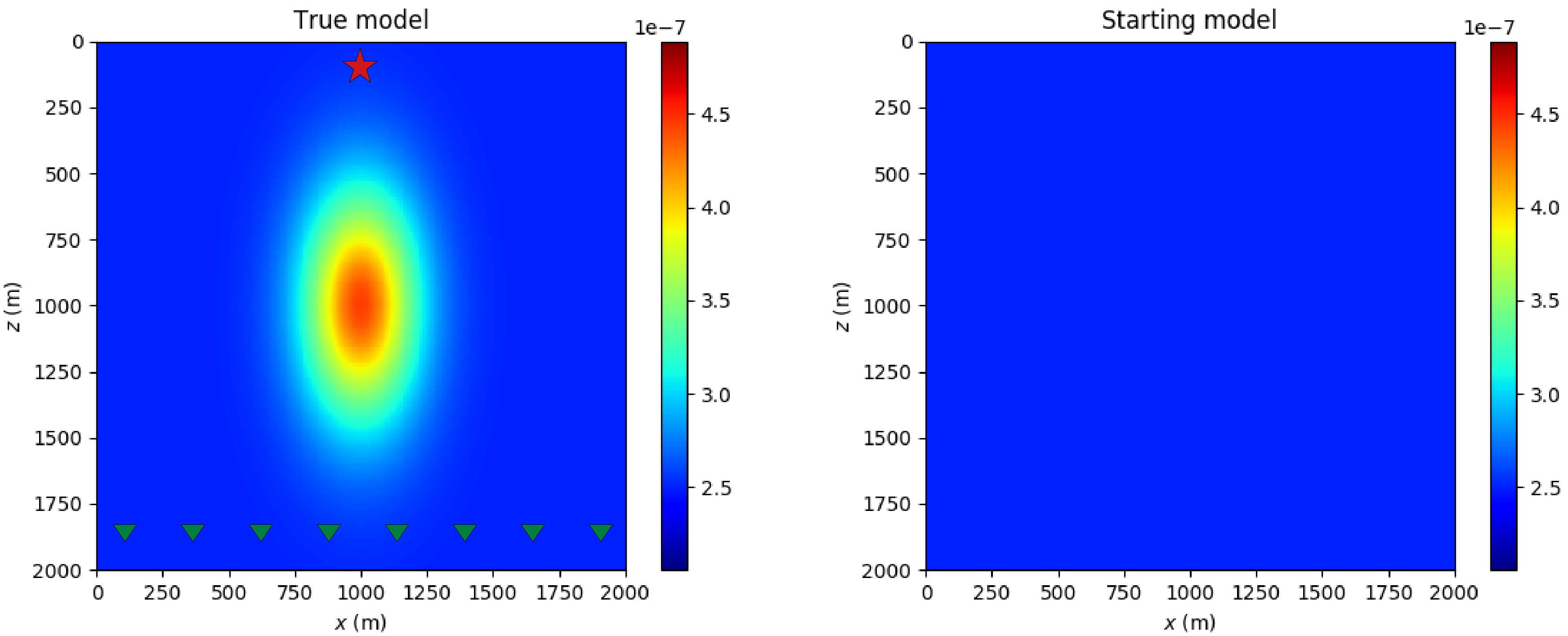


| | |
|---|---|
| Source/receiver configuration: | 50 sources (top), 200 receivers (bottom) |
| Optimization strategy: | Single frequency (6 Hz, wavelength ~ 333 m), Algorithm: L-BFGS (20 iters) |

# Numerical examples – Gaussian lens [Huang et al, 2018]

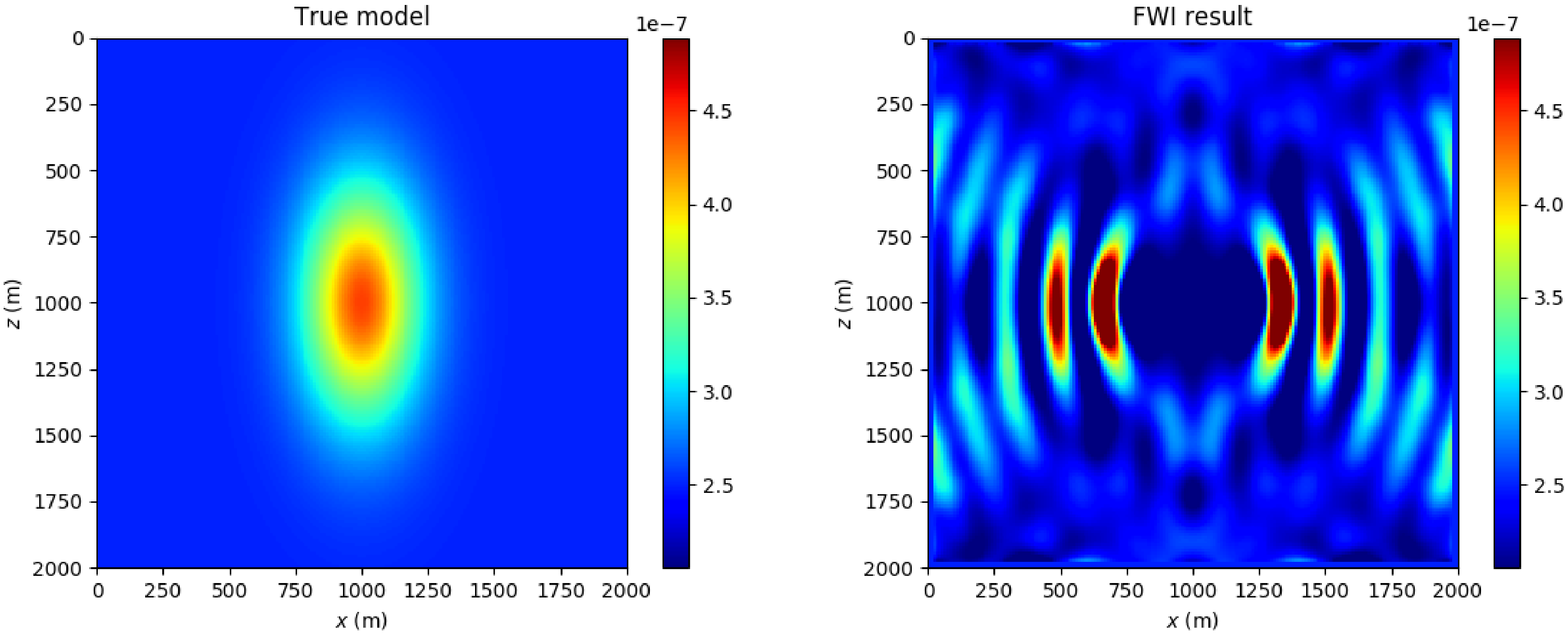


| | |
|---|---|
| Source/receiver configuration: | 50 sources (top), 200 receivers (bottom) |
| Optimization strategy: | Single frequency (6 Hz, wavelength ~ 333 m), Algorithm: L-BFGS (20 iters) |

# Numerical examples – Gaussian lens [Huang et al, 2018]

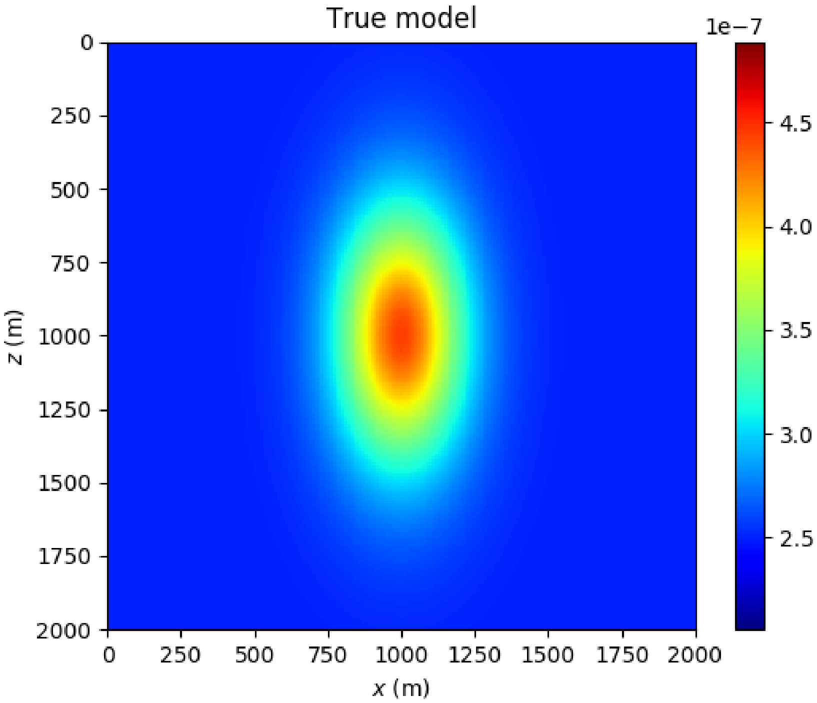


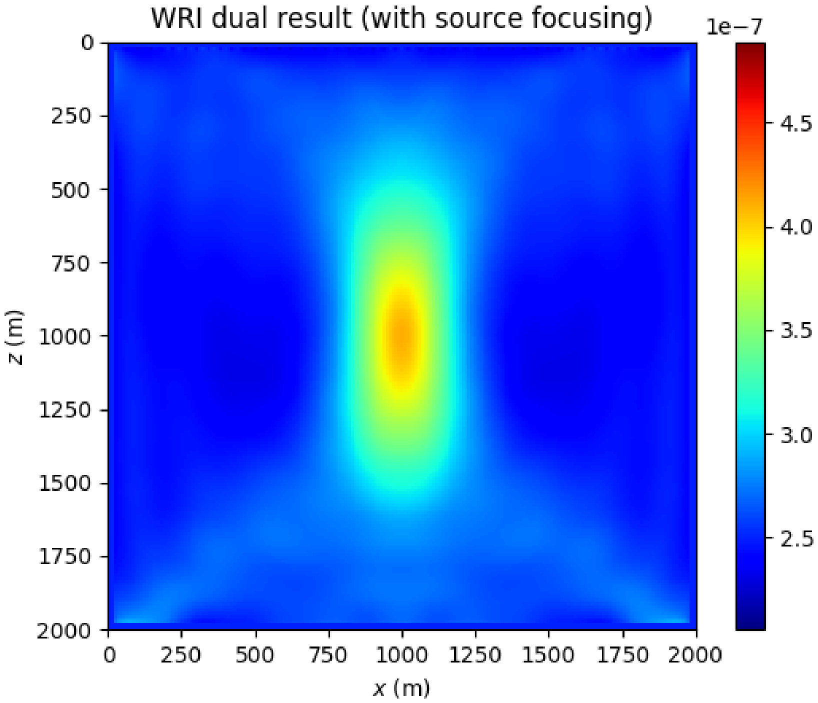


| | |
|---|---|
| Source/receiver configuration: | 50 sources (top), 200 receivers (bottom) |
| Optimization strategy: | Single frequency (6 Hz, wavelength ~ 333 m), Algorithm: L-BFGS (20 iters) |

# Numerical examples – BG Compass model

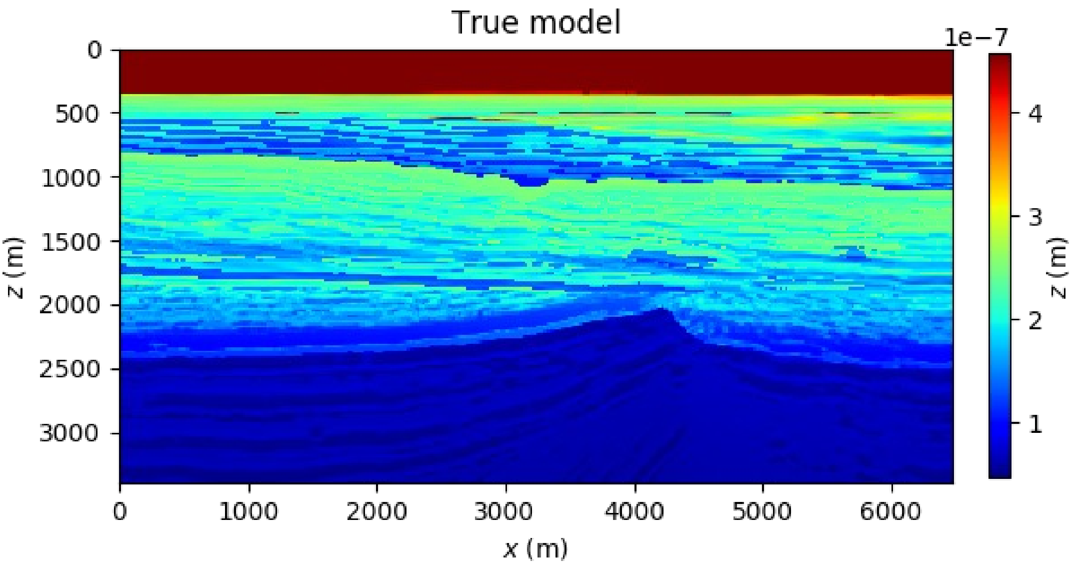


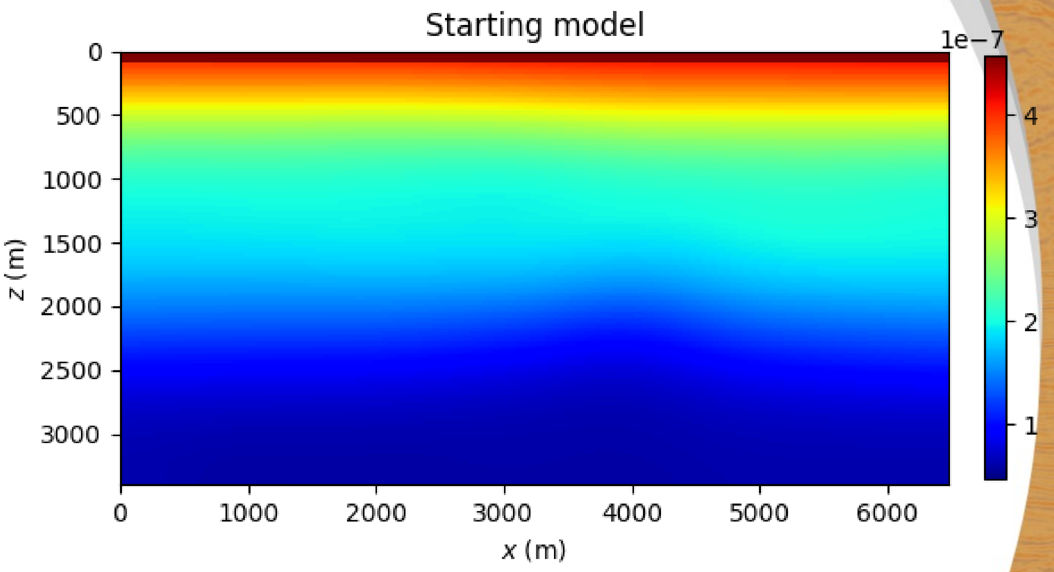


| | |
|---|---|
| Source/receiver configuration: | 50 sources, ~ 300 receivers |
| Optimization strategy: | Multiscale, frequency range: 5 Hz to 14 Hz [2 sweeps], Algorithm: L-BFGS (10 iters) |

# Numerical examples – BG Compass model

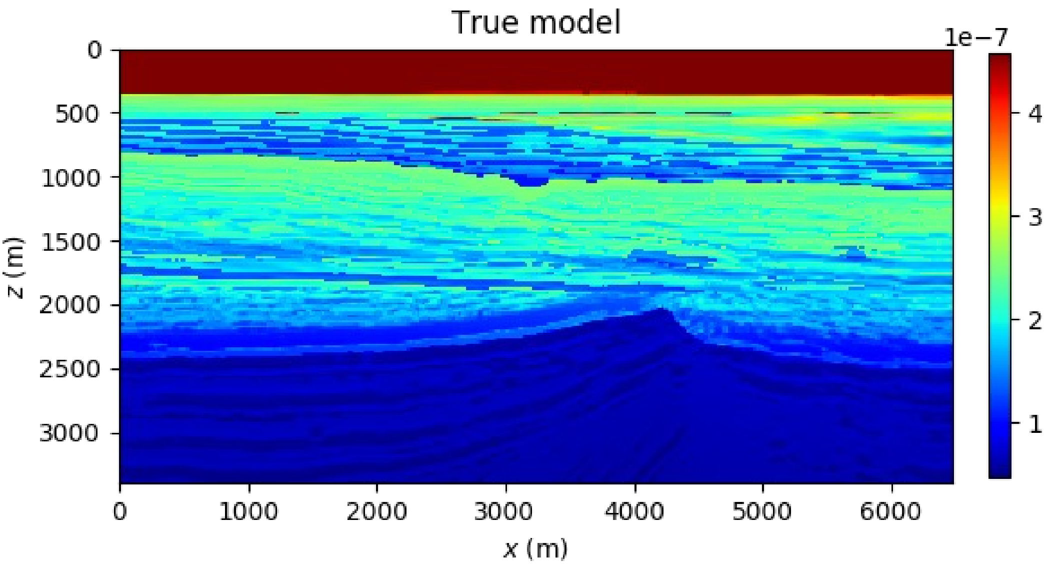


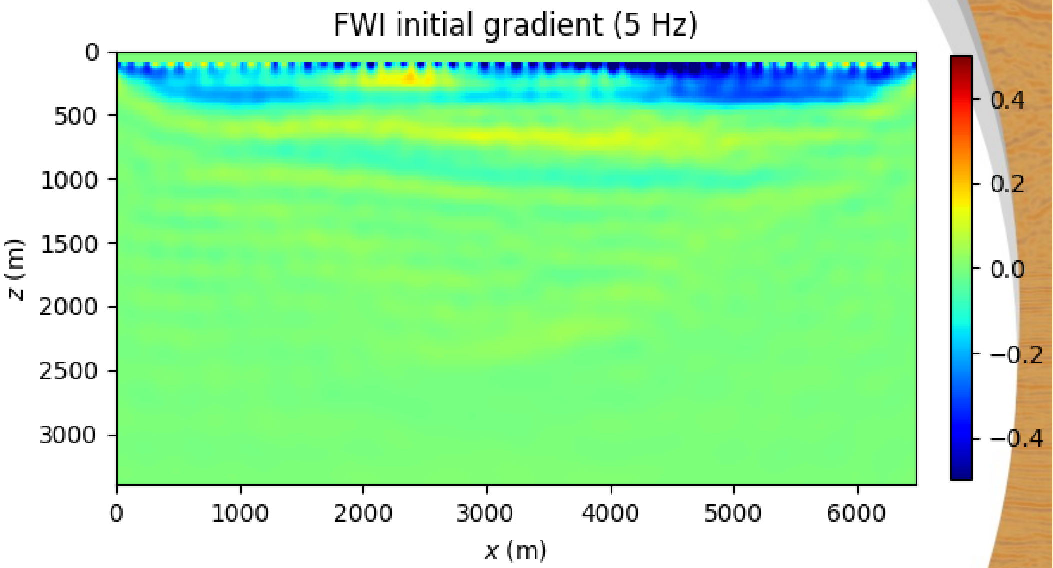


| | |
|---|---|
| Source/receiver configuration: | 50 sources, ~ 300 receivers |
| Optimization strategy: | Multiscale, frequency range: 5 Hz to 14 Hz [2 sweeps], Algorithm: L-BFGS (10 iters) |

# Numerical examples – BG Compass model

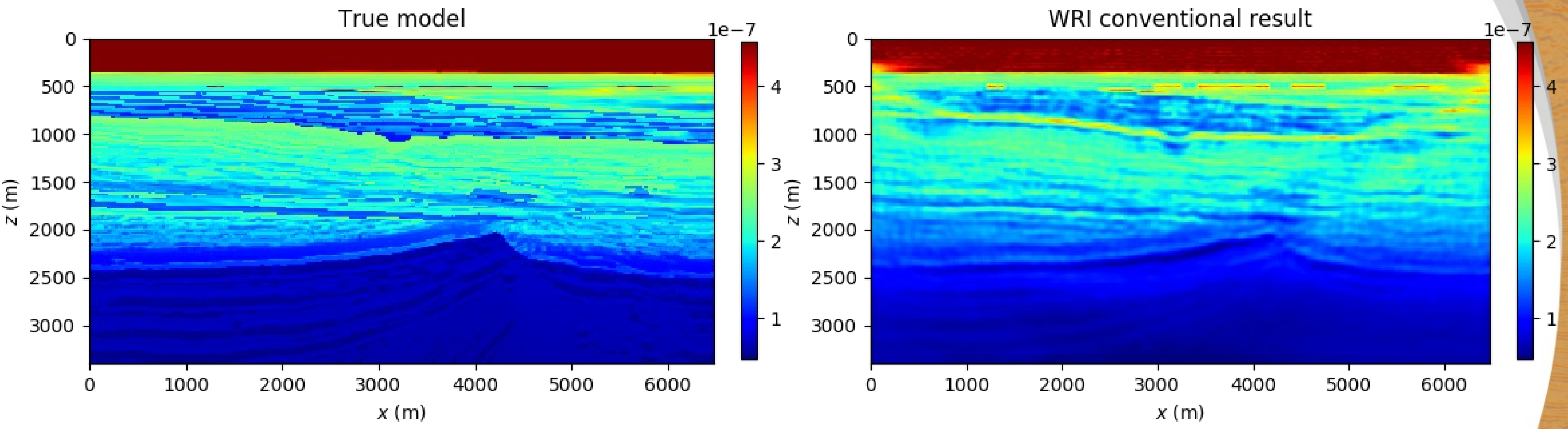


| | |
|---|---|
| Source/receiver configuration: | 50 sources, ~ 300 receivers |
| Optimization strategy: | Multiscale, frequency range: 5 Hz to 14 Hz [2 sweeps], Algorithm: L-BFGS (10 iters) |

# Numerical examples – BG Compass model

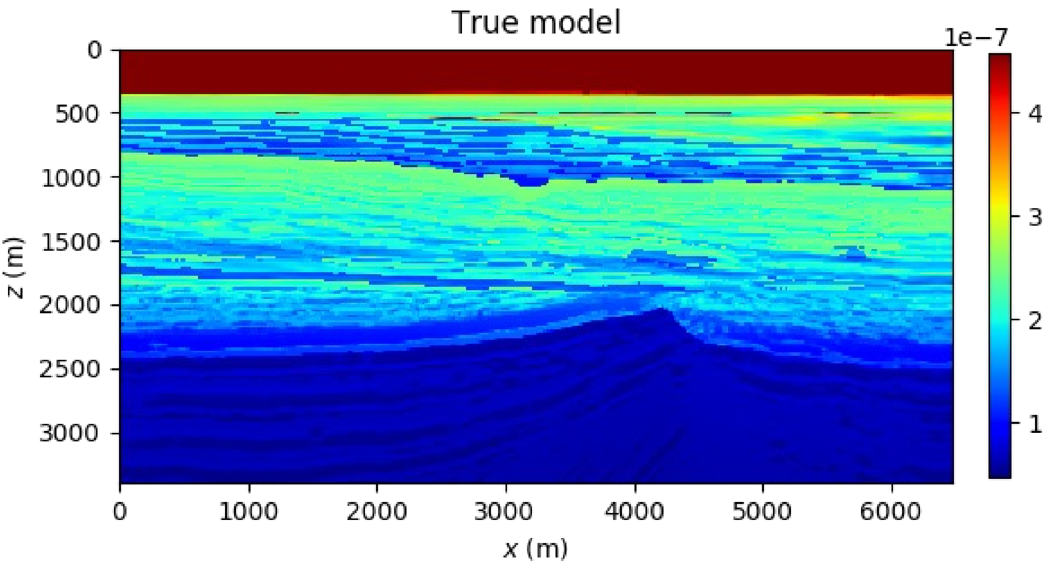


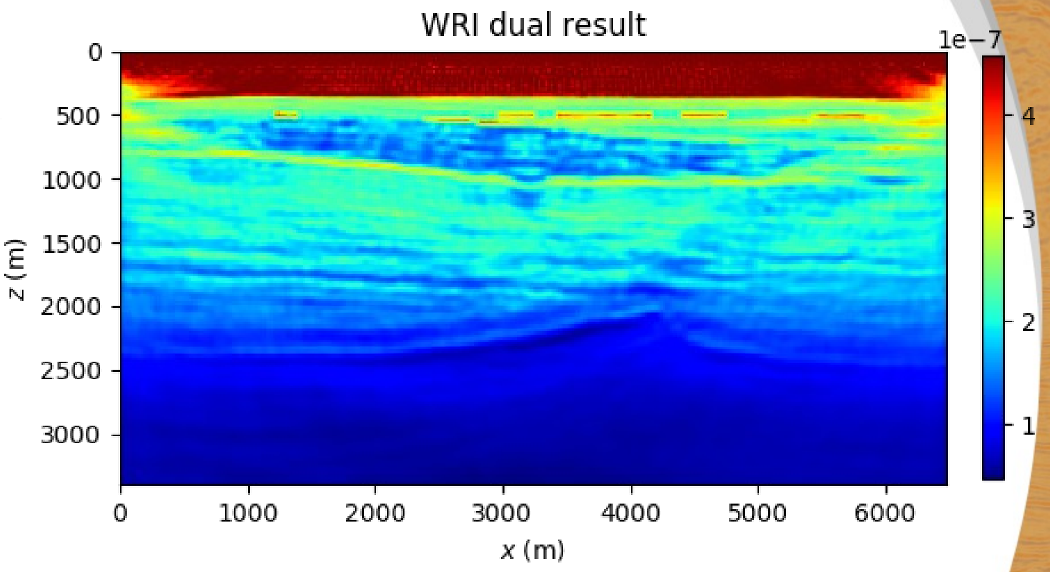


| | |
|---|---|
| Source/receiver configuration: | 50 sources, ~ 300 receivers |
| Optimization strategy: | Multiscale, frequency range: 5 Hz to 14 Hz [2 sweeps], Algorithm: L-BFGS (10 iters) |

# Numerical examples – Marmousi model

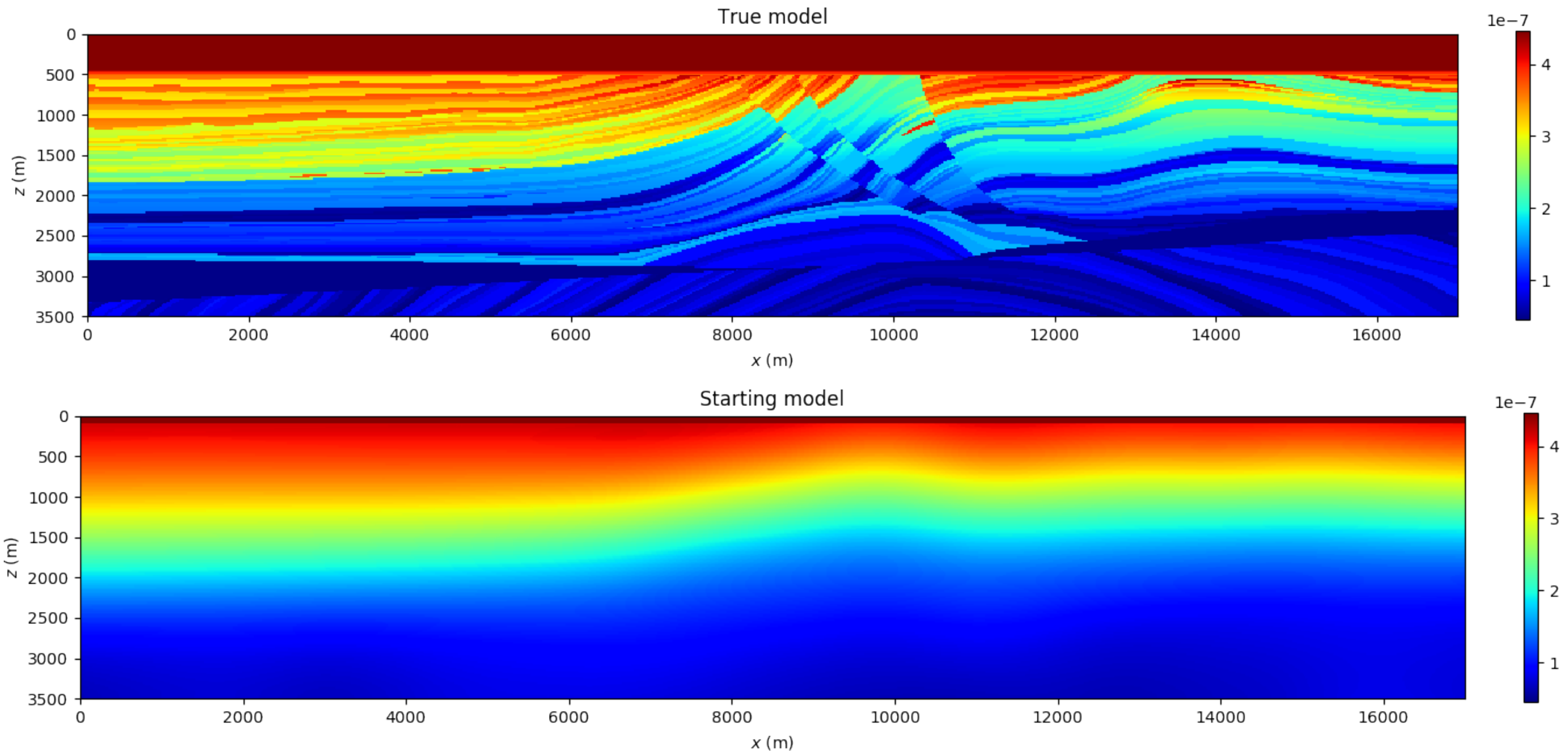


| | |
|---|---|
| Source/receiver configuration: | 100 sources, ~ 850 receivers |
| Optimization strategy: | Multiscale, frequency range: 3 Hz to 14 Hz [2 sweeps], Algorithm: L-BFGS (10 iters) |

# Numerical examples – Marmousi model

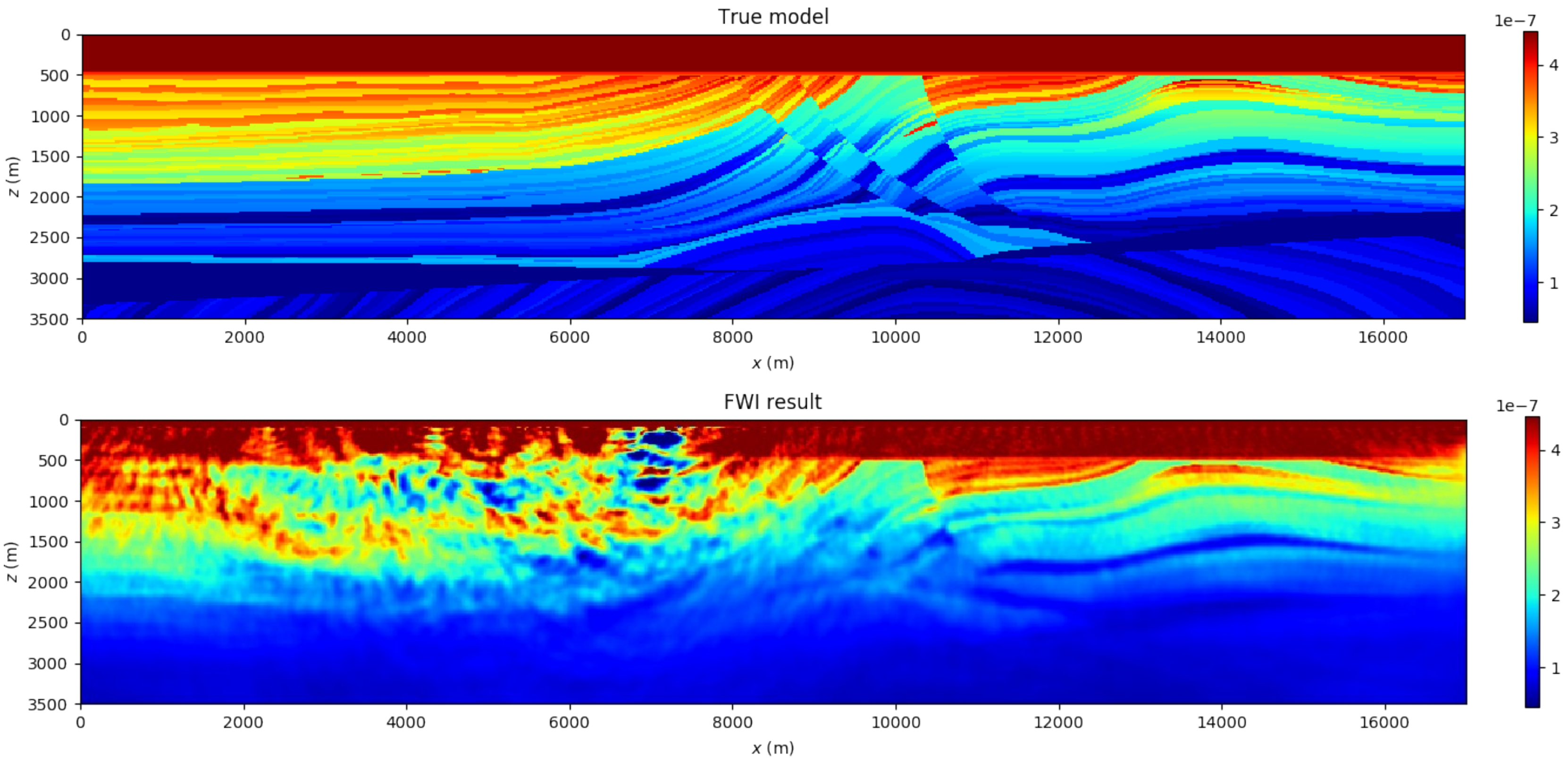


| | |
|---|---|
| Source/receiver configuration: | 100 sources, ~ 850 receivers |
| Optimization strategy: | Multiscale, frequency range: 3 Hz to 14 Hz [2 sweeps], Algorithm: L-BFGS (10 iters) |

# Numerical examples – Marmousi model

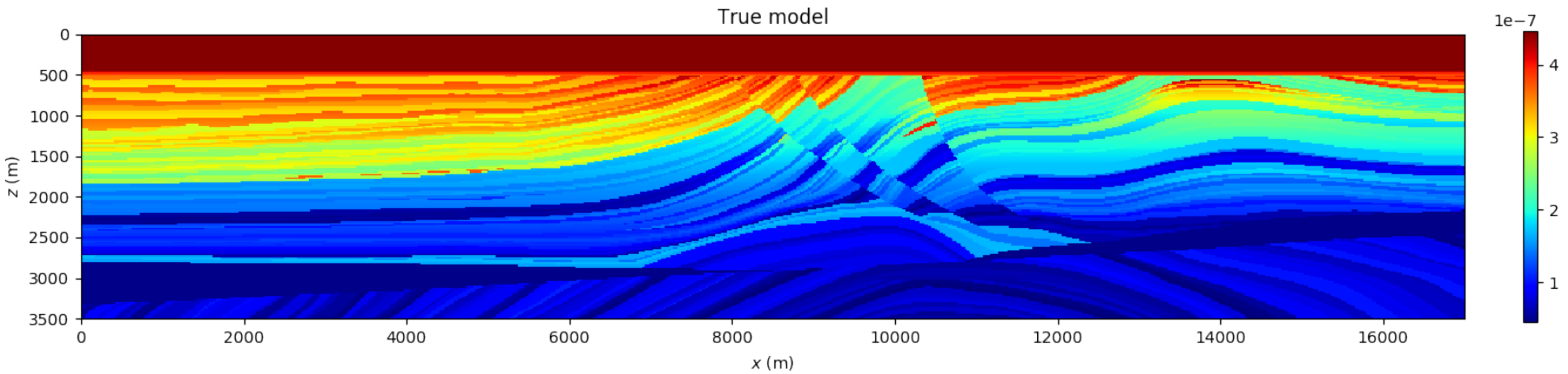


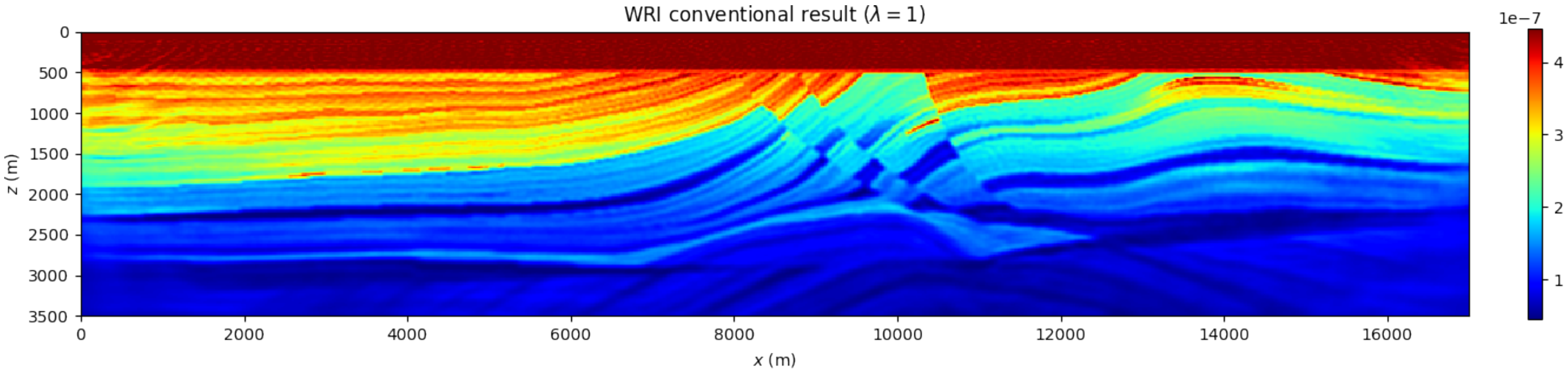


| | |
|---|---|
| Source/receiver configuration: | 100 sources, ~ 850 receivers |
| Optimization strategy: | Multiscale, frequency range: 3 Hz to 14 Hz [2 sweeps], Algorithm: L-BFGS (10 iters) |

# Numerical examples – Marmousi model

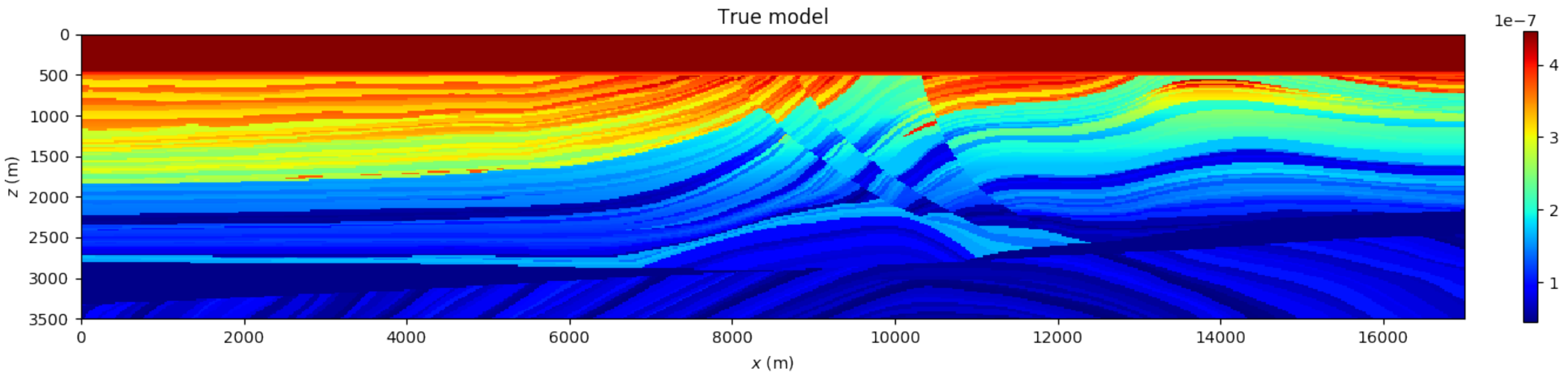


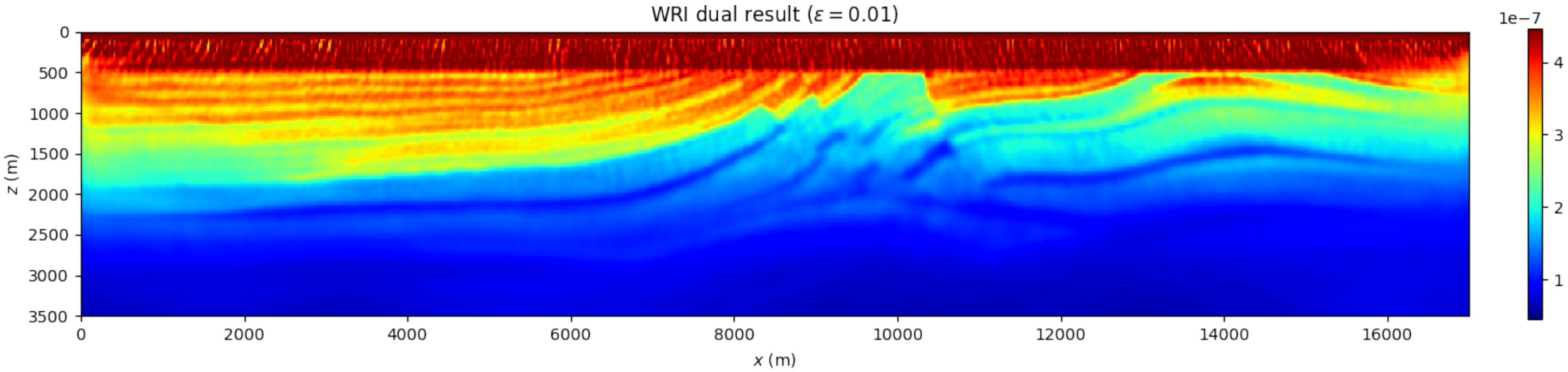


| | |
|---|---|
| Source/receiver configuration: | 100 sources, ~ 850 receivers |
| Optimization strategy: | Multiscale, frequency range: 3 Hz to 14 Hz [2 sweeps], Algorithm: L-BFGS (10 iters) |

# Numerical examples – Marmousi model

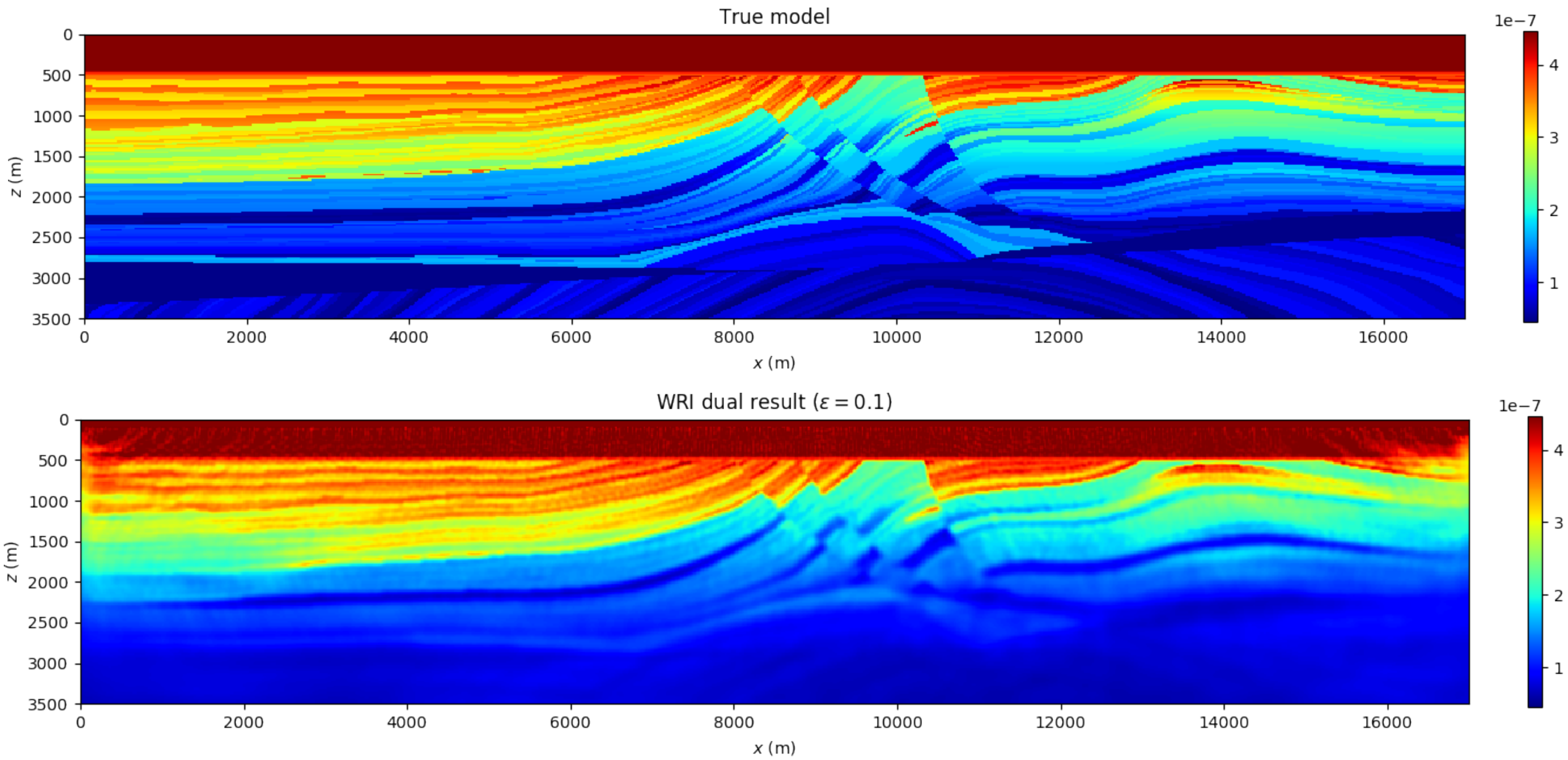


| | |
|---|---|
| Source/receiver configuration: | 100 sources, ~ 850 receivers |
| Optimization strategy: | Multiscale, frequency range: 3 Hz to 14 Hz [2 sweeps], Algorithm: L-BFGS (10 iters) |

# Conclusions and road ahead

Reconstruction algorithm potentially apt to large **3D** problems:

- based on “partial” projection of slack variables
- computational properties: can scale to 3D (unlike WRI!), but 2X FWI
- reconstruction quality: more robust to local minima wrt FWI, but inferior results compared to WRI

What’s next:

- time-domain implementation (almost ready)
- TTI acoustic (M. Louboutin)
- implement constraints, checkpointing, …

# Time-domain implementation details: Devito/JUDI

**Devito**:

domain specific language for stencil-based finite-difference C code generation for PDEs w/ explicit time stepping in *Python* using SymPy

[Luporini et al., 2018; Louboutin et al., 2018]

https://www.devitoproject.org

**JUDI**:

Julia Devito inversion framework: Julia package based on Devito, high-level abstraction of the linear algebra involved in FWI, WRI, … (data vectors, restriction/injection operators, wave equation solution, forward modeling Jacobian and relative adjoint, …)

[Witte et al., 2019]

https://github.com/slimgroup/JUDI.jl

# Open source frequency-domain implementation

Frequency-domain implementation in Julia:

https://github.com/slimgroup/Software.rizzuti2019SEGadf

# References


Biros, G., and Ghattas, O., Parallel Lagrange-Newton-Krylov-Schur methods for PDE-constrained optimization. Part i: The Krylov-Schur solver, SIAM Journal on Scientific Computing, 27 (2005)

Epanomeritakis, I., and Akcelik, V., and Ghattas, O., and Bielak, J., A Newton-CG method for large-scale three-dimensional elastic full-waveform seismic inversion, Inverse Problems, 24(3) (2008)

Grote, M. J., and Huber, J., and Schenk, O., Interior point methods for the inverse medium problem on massively parallel architectures, Procedia Computer Science, 4 (2011)

Haber, E., and Ascher, U. M., and Oldenburg, D., On optimization techniques for solving nonlinear inverse problems, Inverse Problems, 16 (2000)

Haber, E., and Ascher, U. M., Preconditioned all-at-once methods for large, sparse parameter estimation problems, Inverse Problems, 17 (2001)

Huang, G., and Nammour, R., and Symes, W. W., Volume source-based extended waveform inversion, Geophysics (2018)

Kleinman, R. E., and van den Berg, P. M., A modified gradient method for two-dimensional problems in tomography, Journal of Computational and Applied Mathematics, 42 (1992)

van Leeuwen, T., and Herrmann, F. J., Mitigating local minima in full-waveform inversion by expanding the search space, Geophysical Journal International 195.1 (2013)

van Leeuwen, T., A note on extended full waveform inversion, Geophysical Journal International (2019)

Louboutin, M., Lange, M., Luporini, F., Kukreja, N., Witte, P. A., Herrmann, F. J., Velesko, P. and Gorman, G. J., Devito: an embedded domain-specific language for finite differences and geophysical exploration, CoRR, abs/1808.01995, , arXiv (2018)

Luporini, F., Lange, M., Louboutin, M., Kukreja, N., Hückelheim, J., Yount, C., Witte, P., Kelly, P. H. J., Gorman, G. J. and Herrmann, F. J., Architecture and performance of Devito, a system for automated stencil computation, CoRR, abs/1807.03032, 2018, , arXiv (2018)

Peters, B., and Herrmann, F. J., and van Leeuwen, T., Wave-equation Based Inversion with the Penalty Method-Adjoint-state Versus Wavefield-Reconstruction Inversion, 76th EAGE Conference (2014)

Sharan, S., and Wang, R., and Herrmann, F. J., “Fast sparsity-promoting microseismic source estimation”, Geophysical Journal International (2019)

Tarantola, A., Inversion of seismic reflection data in the acoustic approximation, Geophysics 49(8) (1984)

Wang, C., and Yingst, D., and Farmer, P., and Leveille, J., Full Waveform Inversion with the Reconstructed Wavefield Method, 86th EAGE Conference (2016)

Wang, R., and Herrmann, F. J., A denoising formulation of Full-Waveform Inversion, 87th SEG International Exposition (2017)

Witte, P. A., M. Louboutin, N. Kukreja, F. Luporini, M. Lange, G. J. Gorman, and F. J. Herrmann, 2019, A large-scale framework for symbolic implementations of seismic inversion algorithms in Julia: Geophysics, 84, 1–60 (2019)